

Printing Sensors on Biocompatible Substrates for Selective Detection of Glucose

Saleem Khan¹, Shawkat Ali¹, Arshad Khan, Bo Wang², Member, IEEE, and Amine Bermak¹, Fellow, IEEE

Abstract—This article presents development of organic electrochemical transistor (OECT) on a cellulose based biocompatible substrate for selective detection of glucose. The cost-effective manufacturing through drop on demand inkjet printing and blade casting techniques are adopted for the development of OECTs at ambient environment. The OECT is designed by printing carbon-based nanocomposite as the source, drain and gate electrodes, whereas for the channel layer, Poly (3, 4-ethylenedioxythiophene) doped with poly(styrene sulfonate) (PEDOT:PSS) is printed. Optical and physical characterizations were performed to investigate the printability, patterns' uniformity, repeatability, and adhesion of the printed structures onto the target substrate. The sensors are tested against specific enzyme i.e. glucose oxidase mixed in a PBS (phosphate buffer saline) solution. Transistor characteristics of the OECTs are determined to find the best coupling parameters for the device test. The optimal coupling parameters i.e. V_{ds} at 0.8V and V_{gs} at 0.7V produced the transconductance i.e. 0.15 mS, in suitable ranges of the device test. Five different concentrations of glucose were tested in the electrolyte solution starting from the 1 μ M and at maximum 100mM, producing a prominent change in the current response i.e. 20% of its initial value. The distinctive current responses for each glucose concentration at an average response time of \sim 15 sec show very promising results for rapid glucose detection. The low-cost fabrication of these printed sensors on biocompatible substrates show favorable results towards deploying these sensors on human bodies for real-time glucose monitoring.

Index Terms—Printed electronics, sensors, OECTs, flexible, biocompatible, organic materials.

I. INTRODUCTION

PRINTED electronics have attracted significant interest in recent years and are considered as key enablers for exciting developments especially in the area of flexible and wearable sensing applications. Fabrication of various functional layers of an electronic device has become much easier task with direct printing technologies [1]–[4]. The additive manufacturing through drop-on-demand inkjet printing has reduced processing steps that makes it an attractive approach for making low resolution devices [5]–[7]. The lower costs of printing systems and materials are the main driving forces for adoption of these techniques by the academic researchers as

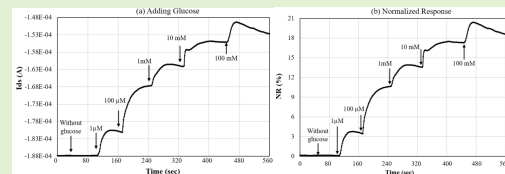
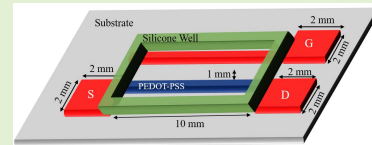
Manuscript received August 10, 2020; revised October 13, 2020; accepted October 13, 2020. Date of publication October 20, 2020; date of current version January 15, 2021. This work was supported by National Priorities Research Program (NPRP) from the Qatar National Research Fund (QNRF) (a member of Qatar Foundation) under Grant NPRP10-0201-170315 and Grant NPRP11S-0110-180246. The associate editor coordinating the review of this article and approving it for publication was Prof. Yu-Cheng Lin. (Corresponding author: Saleem Khan.)

The authors are with the Division of Information and Computing Technology, College of Science and Engineering, Hamad Bin Khalifa University, Doha, Qatar (e-mail: sakhan3@hbku.edu.qa; shaali@hbku.edu.qa; arkhan4@hbku.edu.qa; bwang@hbku.edu.qa; abermak@hbku.edu.qa).

Digital Object Identifier 10.1109/JSEN.2020.3032539

well as in the industry. [5], [8]. Besides the lower prices of printable materials, the location-specific deposition contributes further in lowering the processing cost due to less material wastage [9]. A wide variety of functional materials in their solution form can be processed and deposited on a broad range of flexible, foldable, and stretchable substrates [5], [7]. Many electronic devices have been realized so far as proof of concept and have been applied in real-time applications [10]–[16]. Amongst these, biosensors remain at the heart of these developments, especially for real-time human health monitoring [17]–[19].

The non-invasive detection of various bioanalytes in human body fluids has triggered the development of wearable biosensors and to establish the techniques ideal for these specific applications [18], [20], [21]. Among the various analytes, glucose level detection is one of the widely explored for monitoring the health condition of a diabetic patient [22]–[26]. Conventional testing methods in the medical laboratories are costly, less accessible, and above all involves the collection of blood samples for each test makes the process time consuming and painful for the patients, especially the elder ones. Therefore, interest in the non-invasive and portable diagnostic tools have gained much momentum in recent years, resulting



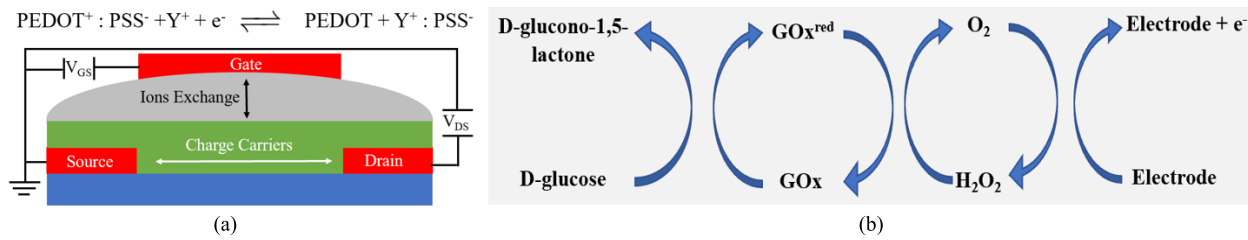


Fig. 1. (a). Working principle, and redox reaction balanced equation of an OEET under an ionic solution, (b). Model redox reaction for enzymatic based electrochemical sensing of glucose.

in the development of wide variety of sensors [22]–[24], [27]. Biosensors based on organic materials are promising due to their low cost, printability as well as biocompatibility make them distinguished from their inorganic counterparts [24], [28].

The three terminal devices i.e. OEETs offer significant advantages for their simple geometric configuration. These devices are easy to manufacture and are able to detect wide variety of analytes selectively by using their respective enzymes [29], [30]. The precise sensing mechanism of OEETs and their development on larger areas provide an easy approach towards improved enzymatic detection. The lower operational voltages i.e. <1 V make OEETs ideal for portable, handheld, and wearable sensing applications [31]. The well-known biocompatible organic conductor i.e. PEDOT-PSS is traditionally used for the active channel, where the doping and dedoping phenomenon occurring in the channel layer in the presence of enzymes-rich electrolyte solution is exploited to detect target analytes [32]. OEETs using PEDOT: PSS as an active channel have already been demonstrated and many have tackled the problem of glucose sensing or tried to analyze sweat [27], [29]. The screen-printed PEDOT-PSS reported on PEN (polyethylene naphthalate) and textile fabric respectively to determine the glucose and different sweat components such as dopamine and ascorbic acid etc. [21], [33], [34]. An inkjet printed OEET is reported utilizing PEDOT-PSS, however silver (Ag) is used for the electrodes [35]. Despite the promising results in these researches, the lack of biocompatible and biodegradable materials as well as the underlying substrates mark a serious challenge. Therefore, this research has targeted the manufacturing of OEETs on cellulose based biocompatible substrate as well as using biocompatible materials for its construction. Besides using PEDOT-PSS as the channel material, carbon-based nanocomposite was used for the source, drain and gate electrodes of the OEET construction. Both the materials are available in solution form and therefore, the cost-effective manufacturing approaches i.e. inkjet printing and blade casting were adopted for patterning the OEET structure. The optical and physical characteristics of the printed structures were evaluated to determine the print quality, adherence of multi-layer structures, reliability, and repeatability of the desired printed patterns. The standard I_{ds} - V_{ds} curves and transconductance characteristics were evaluated to find the best coupling parameters of the device. The electrolyte solution containing glucose oxidase was used to perform the electrochemical analysis at five different concentrations of glucose in the range of $1 \mu\text{M}$ and 100 mM . The electrical and electrochemical analysis showed

very promising results, which can successfully be exploited for wearable and implantable sensing applications.

II. WORKING PRINCIPLE OF OEET

OEETs developed in the early 1980's, are the three terminal devices similar to the standard transistor but with an organic material in place of a semiconductor as the channeling between source and drain electrodes [36]. The gate, however, is connected to the channel material through an electrolyte solution either from top or is developed in co-planar geometries along with source and drain [17], [30], [31]. Fig. 1 shows a schematic diagram of co-planar structure of OEET. The charge carriers are triggered to move in the electrolyte solution corresponding to the applied gate voltage (V_{gs}). This charge variation as a result of V_{gs} causes the doping or dedoping of the channel material and thus changing the current (I_{ds}) between source and drain [28], [30]. The channel material is either functionalized with corresponding sensing material or respective enzymes are mixed in the electrolyte solution for selective detection of a specific analyte. The quantized change in current (I_{ds}) is correlated to the proportional change in the analyte concentration. PEDOT-PSS, an organic conductor is commonly used as channel material in the OEETs' construction [37], [38]. The holes dominant (p-type) PEDOT-PSS is normally-on device having a certain amount of current flowing between the source and drain of the device. In normal conditions, the charge balancing and doping part of the channel materials i.e. PSS makes it more conductive in the absence of a gate voltage (V_{gs}) [30]. However, when a positive voltage is applied at the gate, an increase occurs in the concentration of cations (Y^+ , shown in Fig. 1) existing already in the electrolyte and or generated as a result of the redox reaction after enzymes are added in the solution. These extra positive charges (i.e. Y^+) are injected into the channel material which results in the dedoping of PEDOT-PSS layer⁻. The exact amount of de-doping depends on the potential drop between the electrolyte and the polymer channel, which, in turn, depends on charge transfer reactions that take place at the gate electrode. Commonly in electrochemical sensors, the $\text{O}_2/\text{H}_2\text{O}_2$ couple are often replaced with a fast-redox couple, i.e. ferrocene [bis (n5-cyclopentadienyl) iron] (Fc)/ferricenium ion couple, to overcome the under-consumption issues of oxygen. This facilitating redox couple mediates the rapid transport of electrons from the reduced enzyme to the electrode terminal. However, no mediators are considered in this research due to the reason for exploring the reduced materials' utilization presenting an acceptable range of glucose detection.

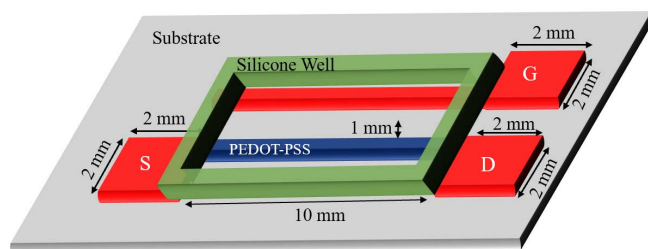


Fig. 2. Schematic diagram of the OEECT and electrolyte containment well with dimensional specification.

As shown in the representative redox reaction of Fig 1 between the enzyme and corresponding analyte, the generated electrons (e^-) move towards the gate electrode, which results in an overall reduction of the current (I_{ds}) flowing between source and drain through EPDOT-PSS channel [23], [27]. Simultaneously, the PEDOT-PSS is reduced, electrons are injected in the channel material resulting into recombination of electrons and holes. The cations present in electrolyte solution partly move in the channel material to ensure the electroneutrality. Since holes are the majority charge carriers in PEDOT-PSS, the channel conductivity is decreased upon increasing the gate voltage. The corresponding change in current (I_{ds}) is directly proportional to the concentration of respective analyte added in the electrolyte solution.

III. DESIGN, MATERIALS AND PROCESSES

A. Design

A co-planar design is selected for fabrication of the OEECT, where all the three electrodes and channel material are patterned on the same surface. Effective area of the sensor is kept large enough to contain sufficient volume of the electrolyte solution for testing. OEECTs are designed according to the previously reported similar structure [35], however this work explores the different aspects by using biocompatible materials and substrates, a step further towards realizing wearable human body worn sensors. The larger dimensions of the device i.e. few millimeters (mm) wide make it interesting for fabricating these sensors through nonconventional manufacturing techniques such as inkjet printing. The demonstrated OEECTs have been reported to perform successfully with dimensions as 10mm long PEDOT-PSS channel at a 1mm spacing from the gate electrode. Fig. 2 shows schematic diagram of the OEECT, representing all the geometric parameters. A containment well to keep the electrolyte solution from flowing out during test defines the active sensing area, as it would be placed such that to prevent contact between ionic solution and the contacting pads. Dimensions of the containment well yielded an active area of $8 \times 6 \text{ mm}^2$ and a thickness of 2mm, that could contain a total volume of 0.096 mL.

B. Substrate

Substrates play an important role in the design of experiments and processing conditions as well as the final application scenarios are based on their physical, thermal, and electrical properties etc. Besides the various important parameters in adopting a polymer-based substrate for flexible electronics,

most important is their glass transition temperatures (T_g). T_g of a substrate determines the suitable materials to be processed and sintered upon at the end of manufacturing process. Therefore, a wide variety of polymer substrates have been developed offering different set of properties for various applications. This research employs biocompatible and biodegradable substrates i.e. Clarifoil obtained from Celanese (UK). The Clarifoil substrates are cellulose acetate films, suitable for the biosensing applications due to their biocompatibility and degradability. The $50\mu\text{m}$ thick substrate was selected for the printing experiments. Substrate were cleaned with deionized (DI) water followed by a dehydration step. A UV ozone treatment was performed for 3 minutes before printing.

C. Electrodes and Channel Materials

Carbon is a biocompatible material and has been used for developing electrodes for biosensors by many researches [39]–[41]. Carbon black was purchased from Sigma Aldrich (product no 699624) and mixed in ethylene glycol at $\sim 40 \text{ wt.}\%$. The synthesized solution has a viscosity of $\sim 25 \text{ cP}$, which is in the suitable range for doctor blade coatings. PEDOT-PSS is an intrinsic p-type material and is commonly used for creating transparent electrodes in various thin film devices such as OLEDs, solar cells, and phototransistors etc. PEDOT-PSS is a promising material available in the solution form at specific rheological properties suitable for inkjet printing. PEDOT-PSS has been procured from Sigma Aldrich synthesized especially for inkjet printing and was used without any further modifications.

D. Electrolyte Solution

Phosphate Buffer Saline (PBS) is the commonly used ionic solution for testing biosensors as it replicates the human body fluid. PBS solution is prepared in DI water in such a way that it matches the salts concentrations similar to those of found in the human body fluids. A weight per volume solution was prepared by mixing 0.8g of PBS in 42g of DI water. For selective detection of glucose, respective enzymes such as glucose oxidase (Sigma-Aldrich (G7141) at 0.1mg/mL is added to the PBS solution.

E. Printing Experiments

The widely practiced printing methods through contact-based and contact-less have provided the opportunity to process a large variety of organic and inorganic materials. Compared to the contact-based printing where desired structures are designed on the printing tools, contact-less printing offers more advantages in terms of rapid design changes, versatility, customization, and re-structuring of the whole manufacturing cycle in a much cost-effective way [1]. Among the various techniques, drop on demand inkjet printing and blade casting are prominent and widely reported, due to their ease in processing, handling of a wide range of materials and above all the lower principle cost of the system. Drop-on-demand inkjet printing is driven by a piezo actuation mechanism where the functional materials in their solution

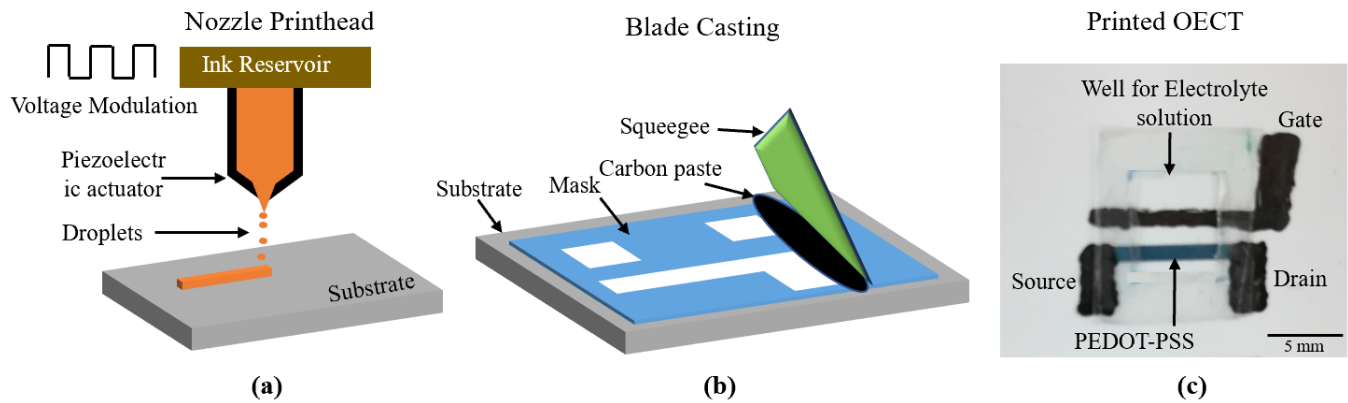


Fig. 3. (a). Schematic of piezoelectric inkjet printing, (b). drop casting, (c) Fabricating device with containment well filled with electrolyte solution.

form are ejected as microdroplets at each corresponding pulse. Fig. 3 (a) shows schematic diagrams of the inkjet printing mechanism. Volume of the droplets is partly dependent on the rheological properties such as viscosity, surface tension, average particle size and vaporization points of the surfactants. Process related control parameters that have a direct bearing on the volume and speed of the droplet generation include the piezoelectric actuation controlled by pulsating waveforms, voltages, jetting frequencies, meniscus set-point, orifice size of the nozzle and the stand-off distance of printhead from the target substrate. The drop to drop spacing is adjusted in such a way that a regular and uniform pattern size is achieved after completing the printing and sintering procedures.

The optimized printing parameters and conditions were set to pattern PEDOT-PSS as the channel layer to connect source and drain of the OECT. Length and width of the channel layer were kept at 12 mm and 1 mm respectively. A 10 pL (picolitre) nozzle printhead (containing 16 nozzles) was used for printing PEDOT-PSS by using DMP-2850 inkjet printing system. The pre-determined printing parameters such as jetting waveform, drop velocity (7mm/sec), platen temperature (at 35°C), jetting frequency of 2kHz, stand-off at 500 μ m and drop-to-drop spacing at 30 μ m were selected in the Dimatix drop manager software. To enhance the electrical conductivity and adhesion to the underlying polymer substrate, six printing cycles were executed (wet-on-dry deposition protocol) at 2 minutes inter-layer delay. Curing of the printed layer was performed at 60 °C overnight, while keeping substrates on the printing platen under vacuum.

Doctor blade coating is used to printed source, drain, and gate electrodes. The blade coating technique is advantageous as it is more versatile, processing is simple and capable of reproducing similar structures in large batches. The shadow mask was prepared through laser etching of a thick plastic sheet. Spacing between the source and drain is kept at 10 mm whereas, gate electrode is printed 1mm apart from the channel. Fig. 3 (b) shows schematics of the mask used for printing the electrodes. The plastic sheet used for shadow mask have thickness of 150 μ m, which is essential for deposition of a thick layer on target substrate. Temperature of the platen was kept at 50° for uniform distribution of the carbon paste as well as rapid evaporation of the surfactants from the

deposited layers. Two coating layers of carbon were executed with an interlayer delay of 15 minutes, allowing a wet-on-dry deposition. After soft baking on the hot platen, samples were cured in oven at 60 °C overnight. Fig. 3(c) shows the fabricated devices after developing the containment well filled with an electrolyte solution.

IV. RESULTS AND DISCUSSIONS

A. Printing Results: Physical and Electrical Characteristics

Quality of the printed structures influences physical, mechanical, and electrical properties of the sensing devices. OECTs are solution-based testing devices, therefore physical adherence of the printed structures to the substrate need particular consideration. Optical micrographs of the printed device show less dimensional variations as shown in Fig. 3(c). The minor variations of few micrometers occurring only in the electrodes are negligible as the size of the device is large and have negligible effect on sensor performance. Scanning electron microscopy (SEM) images of the printed thin films of Carbon and PEDOT-PSS are shown in Fig. 4. Thin films were analyzed at different scales to ensure the uniformity and materials distribution of the printed materials. Figure 4 (a & b) shows carbon black SEM image at 10 and 1 μ m scales, respectively. Similarly, Fig. 4 (c & d) shows SEM images of PEDOT-PSS printed film at 1 μ m and 100 nm scales. The SEM micrographs for both the deposited materials show uniformly printed layers with no cracks after curing.. Adhesion-loss test of the printed films to the polymeric substrate is of prime importance, as upon interaction with the liquid medium during device test, could lead to delamination of the printed structures. Especially in the case of PEDOT-PSS, which comes in direct contact with the electrolyte solution. Therefore, an adhesion-loss test was conducted consecutively after initial curing step of PEDOT-PSS followed by final curing after carbon coating. A scotch tape test was applied to check the attachability of both the films. The presence of cellulose allows partly absorption of the printed ink in the substrate bulk, which also plays significant role in enhancing the adhesion. The multiple printing steps and wet-on-dry deposition also enhanced adhesion of both the surfaces. Electrical properties of both the layers were recorded using a digital multimeter.

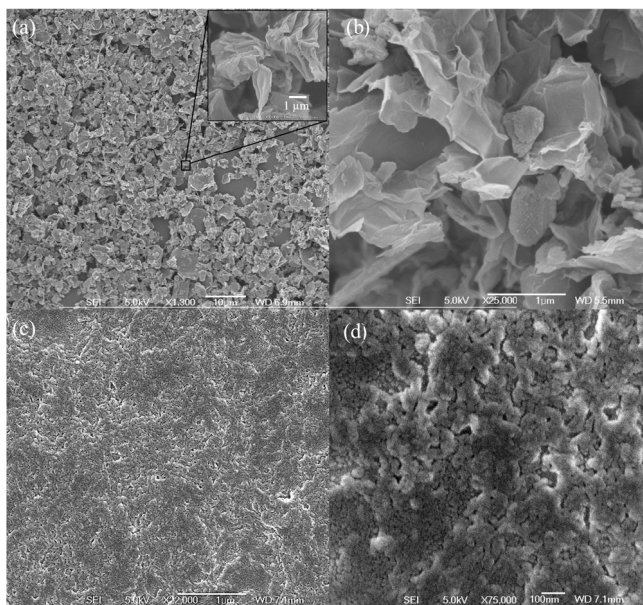


Fig. 4. SEM images of (a & b). Carbon printed films, (c & d). PEDOT-PSS printed films.

Electrical resistance of the PEDOT-PSS channel can be tuned by varying the number of printing layers. Herein, the number of layers is kept higher i.e. 6 in order to keep the conductivity in the desired range within 500 ohms. Despite curing at lower curing temperatures of 60 °C (compared to typical 120°C), the higher number of printing cycles and prolonged overnight curing produces the desired conductivities. Resistance of the PEDOT-PSS layer recorded was ~ 410 ohms, whereas for the carbon-based electrodes, sheet resistance of $45\Omega/\text{sq}$. was recorded.

B. Electrochemical Testing

The electrochemical measurements were performed using a semiconductor parameter analyzer. To confine the electrolyte solution in the effective sensing area with PEDOT-PSS channel layer, a silicone based rectangular shaped containment well was created, as shown in the Fig. 3 (c). Geometric parameters such as thickness, width and length of the containment well were kept as 2 mm, 6mm and 8 mm, respectively. The length and width were designed in such a way to cover the whole effective channel area as well as completely overlapping the pads to avoid direct electrical contact between the electrodes through ionic solution. This well was sufficient enough to contain a considerable volume (100 μL) of the electrolyte solution. An initial amount of 50 μL enzymatic solution (PBS:GOx at mixing ratio of 1:7) was added into the well. The saturated glucose solution was prepared and added into the electrolyte in a way to test six different dilutions, in the range of 1 μM to 100 mM. The sampling frequency is important to determine, as it allows sufficient time to record the changing data occurring as a result of relatively slower biological reactions. Therefore, a measurement delay of 0.5 sec was applied between each sampling event and Ids-Vds curve was determined according to these settings as well. The sweeping

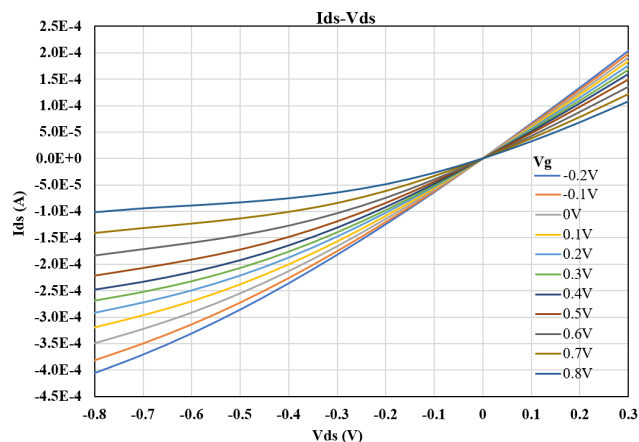


Fig. 5. Ids-Vds curve of the OEETs after filling the containment well with electrolyte solutions.

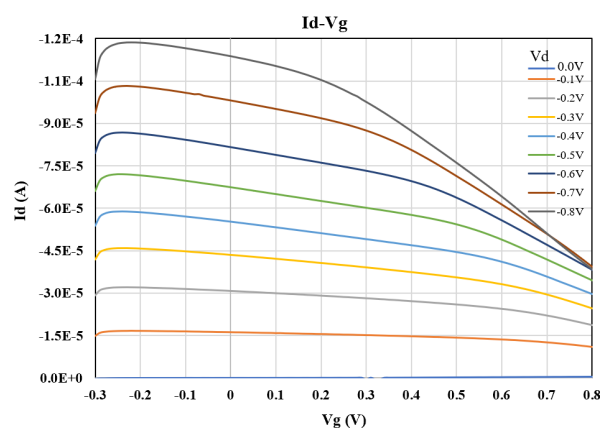


Fig. 6. Ids-Vgs curve of the current response of OEET with electrolyte added in the containment well.

parameters for Ids-Vds curves i.e. Vgs were kept varying from -0.2 to 0.8 V with a 0.1 V step, whereas Vds was swept from -0.8 to 0.3 V with a 0.1 step interval. This combination resulted in 11 data points of Vds being measured at a given value of Vgs and a total of $11 \times 10 = 111$ values, for a single Ids-Vds curve. Sensors were probed and data was acquired starting from dry channel, adding electrolyte, and subsequently adding specific glucose concentrations in the electrolyte solution.

C. Transfer and Transconductance Measurements

The transistor characteristics of the printed sensors were analyzed by obtaining Ids-Vds and transconductance curves. The Ids-Vds curves were analyzed by sweeping the drain voltage (Vds) and gate voltage (Vgs) at a specific frequency, whereas keeping the source grounded. Fig. 5 shows Ids-Vds response at different gate voltages (ranging from -0.2 V to 0.8 V) of transistor with a clearly reaching the saturation regime. The maximum drain current (Ids) in the range of 0.1 mA was recorded in the saturation regime at the peak gate voltage. Upon positive gate voltage, the change in conductivity of the PEDOT-PSS is minimal because of the lesser ionic reactions occurring at the interface of channel layer.

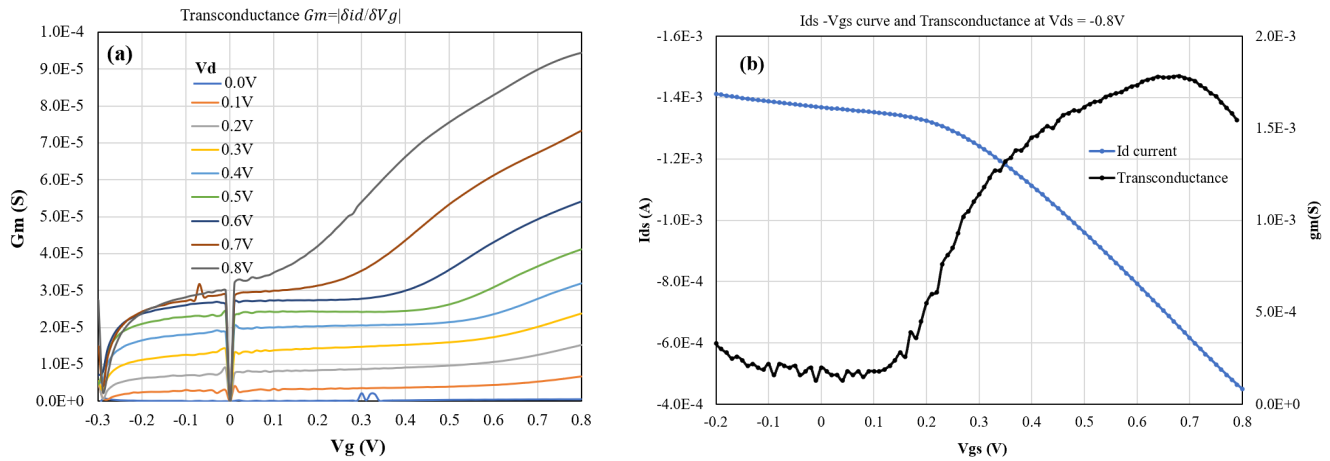


Fig. 7. (a). Transconductance curve of the OEET at different V_{ds} , (b). I_{ds} - V_{gs} curve and transconductance coupling curve at $V_{ds} = -0.8$ V.

These results are in-line with the theory of the operation mechanism of the OEET where an increase in the gate voltage leads to the reduction in current flow in the channel due to the dedoping phenomenon of PEDOT-PSS and increase in drain voltage leads to higher currents till reaching saturation.

To determine the best performance combination from the coupling of V_{ds} and V_{gs} , transconductance (G_m) of the transistor was computed. The G_m was calculated by using the standard formula i.e.

$$G_m = \left| \frac{\delta i_{ds}}{\delta V_{gs}} \right| \quad (1)$$

where δi_{ds} is the rate of change of drain current at corresponding change in the gate voltage. For this measurement, the voltage on the gate V_{gs} was swept with a step 10 times smaller (0.01V) giving more than a 100 values per given V_{ds} . The measured current values shown in Fig. 6, were used to determine the transconductance curve.

The transconductance values accelerate from moderate to higher values at corresponding increasing gate voltages as shown in Fig. 7 (a). The transconductance values were deduced by matching with the variations recorded in the I_{ds} values shown in the graph of Fig. 6. It is evidenced from the plot in Fig. 7 (b), that combination of highest voltage V_{ds} at -0.8 V and V_{gs} at 0.7V gives the highest transconductance i.e. ~ 0.15 mS. The deduced value of G_m is in the acceptable range for such devices. The transconductance value can further be enhanced by tuning the electrical conductivity of the PEDOT-PSS channel layer through post-printing treatments. Combination of these two coupling parameters were used for the electrochemical testing of the sensor against the different concentrations of glucose in the electrolyte solution.

D. Glucose Testing

The electrochemical response of OEET device was analyzed by exposing the sensor in direct contact to the electrolyte solution. The elastomeric well to contain the specific volume of electrolyte was filled and the sensor was probed to record the current response. Prior to testing the glucose concentration, an offset current was recorded with and without the electrolyte solution. Fig. 8 shows the current response of the sensor at

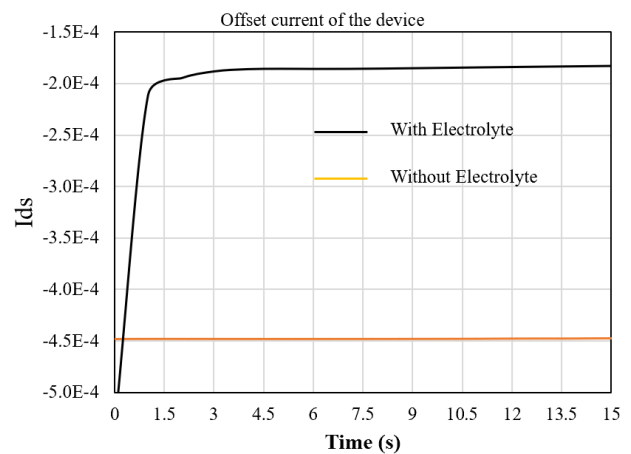


Fig. 8. Offset current of OEET with and without putting electrolyte.

respective testing conditions. It is clear from the graph that drain current increases significantly by adding the electrolyte solution. The ions present in the electrolyte solution interacts with the channel material and modulates the current at higher threshold as compared to the stable current level at dry condition. The rising and stabilization curve of the current response after few seconds determines that a stabilization period is required to reach the saturation regime before adding glucose in the electrolyte. The glucose was added in electrolyte solution such that five different molar concentrations within the range of $1 \mu\text{M}$ to 100 mM were achieved. Fig. 9 (a) shows response of the sensor in terms of current (I_{ds}) increase with each corresponding concentration of glucose added into the electrolyte solution. Fig. 9 (b) shows normalized response of the sensor at each corresponding measurement.

Both the graph shown in Fig. 9 (a & b) show a clear distinction between each consecutive increment of glucose concentrations in the electrolyte solution. The change in current response is $\sim 4\%$ compared to the initial stabilized values at corresponding minimal concentration i.e. $1 \mu\text{M}$. Similarly, for higher glucose concentration i.e. 100 mM , the drain current increases significantly by $\sim 20\%$. These results are congruent to the working principle of OEETs as higher concentrations

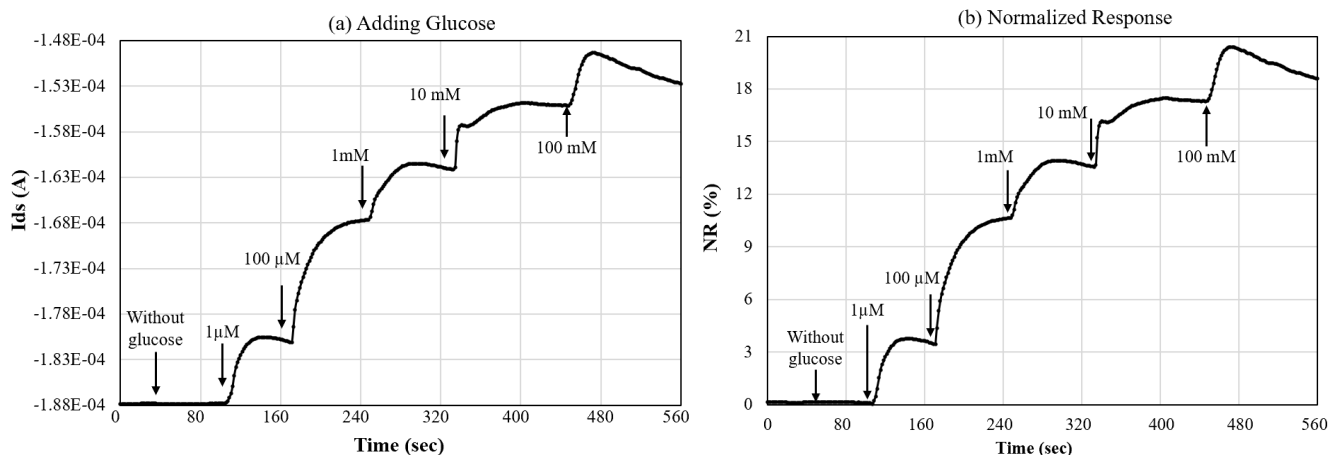


Fig. 9. Sensors response against different glucose concentrations and their normalized response.

provide a higher chance to bind to the enzymes and leading to higher electrons exchanges at the channel. The sensor reaches its stabilization current initially in a short interval ~ 2 minutes, however the interval between successive measurements is minimized till the point they reach saturation. The increase and slight decrease in the current response at each measurement step is caused by the equilibrium between glucose and enzymes present in the electrolyte solution. Ideally the sensor should reach the saturation regime without losses in the current peaks, however this would require the active channel layer to be functionalized with the corresponding enzymes. In this configuration, enzymes are mixed in the electrolyte solution and the glucose can easily unbind. This might be affecting the exchange of electrons between the two molecules and resulting into increase in current across the channel. Nonetheless, these slight variations are acceptable and have insignificant effect on the overall performance of the sensor. The sensor's average response time is also determined i.e. 14 sec, by considering the 60% change in the recorded current as shown in Fig. 10. The response time of the sensor is also in acceptable ranges compared to the commercially available glucose sensors, which give response typically in 5-10 seconds.

Repeatability of the same sensor for multiple tests is ideally required especially when targeting wearable sensing applications. Therefore, the same sensors were undergone for repeated tests at similar testing conditions and very slight variations in the current responses were recorded. These were also confirmed by counter checking the intrinsic resistance of the PEDOT-PSS layer under dry conditions. The electrolyte solution from the containment well was drained out and let the channel material dries under ambient environment. A slight increase of ~ 15 ohms in the initial resistance (410 ohms) of the PEDOT-PSS was recorded, which could possibly be contributed from the insufficient dryness of the layer or residual ions left behind in the channel layer. Five different sensors with similar geometric parameters were tested to replicate the sensors' responses. Fig. 11 shows graph of the standard deviation for the five tested sensors showing negligible variations. The variations were caused by the slight variation in the base resistances, which were mainly contributed from their

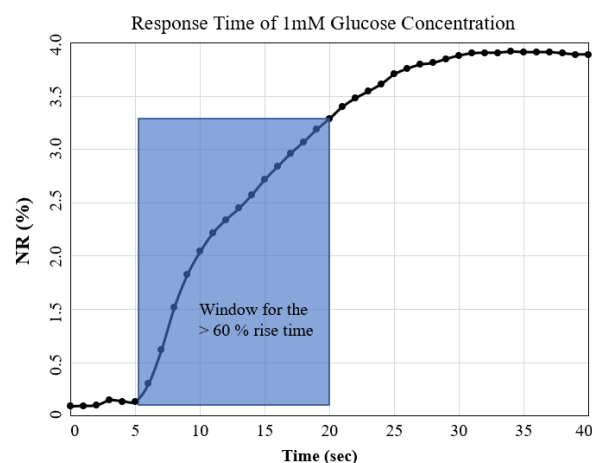


Fig. 10. Response time of the sensor after adding 1mM glucose in electrolyte solution.

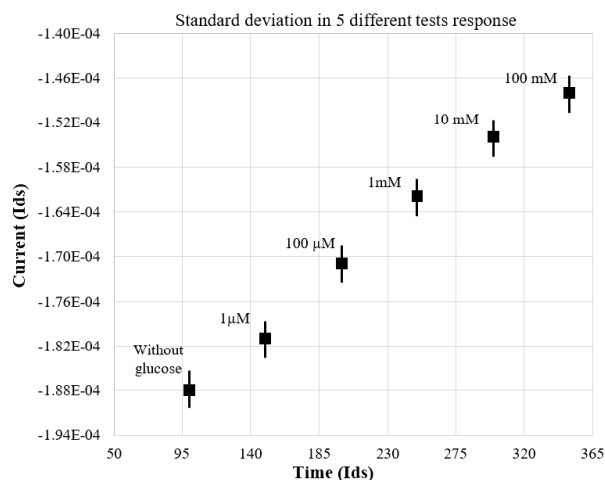


Fig. 11. Standard deviation in responses of 5 different tests performed on a single sensor.

manufacturing through printing. Minimal deviations in the pattern width as well layer thicknesses through solution based printing are obvious, and therefore these characteristics ultimately influence the final results. Nonetheless, these variations

are minimal and can be overcome by proper selection of the printing materials as well as controlled experimental conditions.

V. CONCLUSION

An all-printed OECTs based glucose sensor is fabricated on biocompatible and degradable substrates. The processing parameters for inkjet printing of PEDOT-PSS were optimized aiming to pattern the conducting channel of OECT at desired geometry. An overnight curing was performed by keeping the printed structures at 60 °C resulting into an electrical resistance of 410 Ω. Blade casting of carbon-based paste was performed for patterning source drain and gate electrodes. Reliability of the printed structures was determined by investigating the optical and physical characteristics. The Ids-Vds curves and transconductance characteristics were measured to deduce the best coupling parameters. The electrolyte solution prepared by mixing PBS and glucose oxidase was contained in a well, interfacing the PEDOT-PSS channel and gate electrode. The optimal coupling parameters i.e. Vds at 0.8V and Vgs at 0.7V produced the highest transconductance i.e. 0.15 mS. The different concentrations of glucose were added to the electrolyte solution starting from 1 μM and at maximum 100mM. A significant change in the current response i.e. 20% of its initial value at lower response time of ~15 sec show very promising results. The sensor structure would further be modified, and functionalization of the active area would lead towards wearing these sensors directly on human skin.

REFERENCES

- [1] S. Khan, L. Lorenzelli, and R. S. Dahiya, "Technologies for printing sensors and electronics over large flexible substrates: A review," *IEEE Sensors J.*, vol. 15, no. 6, pp. 3164–3185, Jun. 2015.
- [2] A. Nag, S. C. Mukhopadhyay, and J. Kosel, "Wearable flexible sensors: A review," *IEEE Sensors J.*, vol. 17, no. 13, pp. 3949–3960, Jul. 2017.
- [3] T. Seifert, E. Sowade, F. Roscher, M. Wiemer, T. Gessner, and R. R. Baumann, "Additive manufacturing technologies compared: Morphology of deposits of silver ink using inkjet and aerosol jet printing," *Ind. Eng. Chem. Res.*, vol. 54, no. 2, pp. 769–779, Jan. 2015.
- [4] H. Matsui, Y. Takeda, and S. Tokito, "Flexible and printed organic transistors: From materials to integrated circuits," *Organic Electron.*, vol. 75, Dec. 2019, Art. no. 105432.
- [5] J. Oliveira, V. Correia, H. Castro, P. Martins, and S. Lanceros-Mendez, "Polymer-based smart materials by printing technologies: Improving application and integration," *Additive Manuf.*, vol. 21, pp. 269–283, May 2018.
- [6] S. Ali, S. Khan, and A. Bermak, "Inkjet-printed human body temperature sensor for wearable electronics," *IEEE Access*, vol. 7, pp. 163981–163987, 2019.
- [7] S. Khan, S. Ali, and A. Bermak, "Substrate dependent analysis of printed sensors for detection of volatile organic compounds," *IEEE Access*, vol. 7, pp. 134047–134054, 2019.
- [8] S. Khan, S. Ali, and A. Bermak, "Recent developments in printing flexible and wearable sensing electronics for healthcare applications," *Sensors*, vol. 19, no. 5, p. 1230, Mar. 2019.
- [9] T.-Y. Chu, Z. Zhang, A. Dadvand, C. Py, S. Lang, and Y. Tao, "Direct writing of inkjet-printed short channel organic thin film transistors," *Organic Electron.*, vol. 51, pp. 485–489, Dec. 2017.
- [10] S. Ali, S. Khan, and A. Bermak, "All-printed human activity monitoring and energy harvesting device for Internet of thing applications," *Sensors*, vol. 19, no. 5, p. 1197, Mar. 2019.
- [11] T. Sekine *et al.*, "Fully printed wearable vital sensor for human pulse rate monitoring using ferroelectric polymer," *Sci. Rep.*, vol. 8, p. 4442, Mar. 2018.
- [12] S. Khan, S. Tinku, L. Lorenzelli, and R. S. Dahiya, "Flexible tactile sensors using screen-printed P (VDF-TrFE) and MWCNT/PDMS composites," *IEEE Sensors J.*, vol. 15, pp. 3146–3155, Jun. 2015.
- [13] Y. Seekaew, S. Lokavee, D. Phokharatkul, A. Wisitsoraat, T. Kerdcharoen, and C. Wongchoosuk, "Low-cost and flexible printed graphene-PEDOT:PSS gas sensor for ammonia detection," *Organic Electron.*, vol. 15, no. 11, pp. 2971–2981, Nov. 2014.
- [14] S. Ali, J. Bae, C. H. Lee, K. H. Choi, and Y. H. Doh, "All-printed and highly stable organic resistive switching device based on graphene quantum dots and polyvinylpyrrolidone composite," *Organic Electron.*, vol. 25, pp. 225–231, Oct. 2015.
- [15] J. Chang, X. Zhang, T. Ge, and J. Zhou, "Fully printed electronics on flexible substrates: High gain amplifiers and DAC," *Organic Electron.*, vol. 15, no. 3, pp. 701–710, Mar. 2014.
- [16] S. Khan, S. Tinku, L. Lorenzelli, and R. S. Dahiya, "Flexible tactile sensors using screen-printed P(VDF-TrFE) and MWCNT/PDMS composites," *IEEE Sensors J.*, vol. 15, no. 6, pp. 3146–3155, Jun. 2015.
- [17] Q. Chen *et al.*, "Flexible electrochemical biosensors based on graphene nanowalls for the real-time measurement of lactate," *Nanotechnology*, vol. 28, no. 31, Aug. 2017, Art. no. 315501.
- [18] T. Vuorinen, J. Niittynen, T. Kankkunen, T. M. Kraft, and M. Mäntyselä, "Inkjet-printed graphene/PEDOT:PSS temperature sensors on a skin-conformable polyurethane substrate," *Sci. Rep.*, vol. 6, no. 1, p. 35289, Dec. 2016.
- [19] L. Manjakkal, A. Vilouras, and R. Dahiya, "Screen printed thick film reference electrodes for electrochemical sensing," *IEEE Sensors J.*, vol. 18, no. 19, pp. 7779–7785, Oct. 2018.
- [20] X. Tao, S. Liao, S. Wang, D. Wu, and Y. Wang, "A body compatible thermometer based on green electrolytes," *ACS Sensors*, vol. 3, no. 7, pp. 1338–1346, 2018.
- [21] N. Coppedè *et al.*, "Ion selective textile organic electrochemical transistor for wearable sweat monitoring," *Organic Electron.*, vol. 78, Mar. 2020, Art. no. 105579.
- [22] H. Yoon, X. Xuan, S. Jeong, and J. Y. Park, "Wearable, robust, non-enzymatic continuous glucose monitoring system and its *in vivo* investigation," *Biosensors Bioelectron.*, vol. 117, pp. 267–275, Oct. 2018.
- [23] X. Xuan, H. S. Yoon, and J. Y. Park, "A wearable electrochemical glucose sensor based on simple and low-cost fabrication supported micro-patterned reduced graphene oxide nanocomposite electrode on flexible substrate," *Biosensors Bioelectron.*, vol. 109, pp. 75–82, Jun. 2018.
- [24] S. Soyilemez, H. Z. Kaya, Y. A. Udum, and L. Toppare, "A multipurpose conjugated polymer: Electrochromic device and biosensor construction for glucose detection," *Organic Electron.*, vol. 65, pp. 327–333, Feb. 2019.
- [25] X. Luo, H. Yu, and Y. Cui, "A wearable amperometric biosensor on a cotton fabric for lactate," *IEEE Electron Device Lett.*, vol. 39, no. 1, pp. 123–126, Jan. 2018.
- [26] Y. Aleeva *et al.*, "Amperometric biosensor and front-end electronics for remote glucose monitoring by crosslinked PEDOT-glucose oxidase," *IEEE Sensors J.*, vol. 18, no. 12, pp. 4869–4878, Jun. 2018.
- [27] S. Y. Oh *et al.*, "Skin-attachable, stretchable electrochemical sweat sensor for glucose and pH detection," *ACS Appl. Mater. Interfaces*, vol. 10, no. 16, pp. 13729–13740, Apr. 2018.
- [28] J. Rivnay, R. M. Owens, and G. G. Malliaras, "The rise of organic bioelectronics," *Chem. Mater.*, vol. 26, no. 1, pp. 679–685, Jan. 2014.
- [29] J. Kim, R. Kumar, A. J. Bandodkar, and J. Wang, "Advanced materials for printed wearable electrochemical devices: A review," *Adv. Electron. Mater.*, vol. 3, no. 1, Jan. 2017, Art. no. 1600260.
- [30] J. T. Friedlein, R. R. McLeod, and J. Rivnay, "Device physics of organic electrochemical transistors," *Organic Electron.*, vol. 63, pp. 398–414, Dec. 2018.
- [31] D. A. Bernards and G. G. Malliaras, "Steady-state and transient behavior of organic electrochemical transistors," *Adv. Funct. Mater.*, vol. 17, no. 17, pp. 3538–3544, Nov. 2007.
- [32] S. Kirchmeyer and K. Reuter, "Scientific importance, properties and growing applications of poly (3, 4-ethylenedioxythiophene)," *J. Mater. Chem.*, vol. 15, no. 21, pp. 2077–2088, 2005.
- [33] G. Scheiblin *et al.*, "Screen-printed organic electrochemical transistors for metabolite sensing," *MRS Commun.*, vol. 5, no. 3, pp. 507–511, Sep. 2015.
- [34] I. Gualandri, M. Marzocchi, A. Achilli, D. Cavedale, A. Bonfiglio, and B. Fraboni, "Textile organic electrochemical transistors as a platform for wearable biosensors," *Sci. Rep.*, vol. 6, no. 1, pp. 1–10, Sep. 2016.
- [35] G. Mattana, D. Briand, A. Murette, A. V. Quintero, and N. F. de Rooij, "Polylactic acid as a biodegradable material for all-solution-processed organic electronic devices," *Organic Electron.*, vol. 17, pp. 77–86, Feb. 2015.

- [36] H. S. White, G. P. Kittlesen, and M. S. Wrighton, "Chemical derivatization of an array of three gold microelectrodes with polypyrrole: Fabrication of a molecule-based transistor," *J. Amer. Chem. Soc.*, vol. 106, no. 18, pp. 5375–5377, Sep. 1984.
- [37] S.-M. Kim *et al.*, "Influence of PEDOT: PSS crystallinity and composition on electrochemical transistor performance and long-term stability," *Nature Commun.*, vol. 9, no. 1, pp. 1–9, 2018.
- [38] I. Gualandi, D. Tonelli, F. Mariani, E. Scavetta, M. Marzocchi, and B. Fraboni, "Selective detection of dopamine with an all PEDOT: PSS organic electrochemical transistor," *Sci. Rep.*, vol. 6, p. 35419, Oct. 2016.
- [39] A. Walcarius, "Electrocatalysis, sensors and biosensors in analytical chemistry based on ordered mesoporous and macroporous carbon-modified electrodes," *TrAC Trends Anal. Chem.*, vol. 38, pp. 79–97, Sep. 2012.
- [40] I. Svancara, K. Vyřas, J. Barek, and J. Zima, "Carbon paste electrodes in modern electroanalysis," *Crit. Rev. Anal. Chem.*, vol. 31, pp. 311–345, Oct. 2001.
- [41] J. G. Giuliani, T. E. Benavidez, G. M. Duran, E. Vinogradova, A. Rios, and C. D. Garcia, "Development and characterization of carbon based electrodes from pyrolyzed paper for biosensing applications," *J. Electroanal. Chem.*, vol. 765, pp. 8–15, Mar. 2016.



Saleem Khan received the master's degree in electronic engineering from Jeju National University, South Korea, and the Ph.D. degree in materials science engineering from the University of Trento, Italy. He worked as a Scientific Collaborator at EPFL, Switzerland. He is currently a Postdoctoral Fellow with HBKU, Qatar. He has more than nine years of experience in exploring printable materials and printing technologies. His research interests include development of all printed microelectronic transducers and sensing

devices on polymeric substrates. He also worked on the heterogeneous integration of printing and microfabrication technologies for establishing a single fabrication platform. He has contributed in more than 40 research articles, two patents, and a book chapter on nanomaterials-based printed gas sensors. He was a recipient of various prestigious scholarships like Brain Korea 21st century awards program (BK21), Marie Curie, the Early Stage Researcher Award, and the ERC Fellow Award.

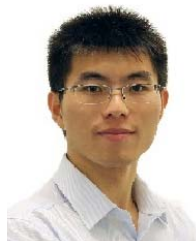


Shawkat Ali received the master's degree from the National University of Computer and Emerging Sciences, Islamabad, Pakistan, in 2012, and the Ph.D. degree from Jeju National University, South Korea, in 2016, all in electrical/electronic engineering. He has been a Postdoctoral Fellow with Hamad Bin Khalifa University, Qatar, since 2017. He was an Assistant Professor with the Department of Electrical Engineering, NU-FAST, Islamabad, from 2016 to 2017. His research

interests include radio frequency electronics, nanotechnology, wearable and implantable electronics, biomedical sensors, resistive memory, and energy harvesting. He has also been involving in research throughout of his professional carrier and published more than 30 research articles, registered eight patents, and graduated three master's students. He has been awarded two times as Productive Scientist by the Pakistan Council for Science and Technology (PCST) from 2016 to 2018.



Arshad Khan received the master's degree in mechatronic engineering from Jeju National University, South Korea, and the Ph.D. degree in mechanical engineering from the University of Hong Kong, Hong Kong. He was a joint Postdoctoral Research Fellow between the Max Planck Institute for Informatics (MPI-Inf), Germany, and the Leibniz Institute for New Materials (Leibniz-INM), Germany. He is currently a Postdoctoral Researcher with the College of Science and Engineering, Hamad Bin Khalifa University, Qatar. His current research focuses on the development of self-powered and soft wearable electronics for human activities and health monitoring.



Bo Wang (Member, IEEE) received the B.Eng. (Hons.) degree in electrical engineering from Zhejiang University, Hangzhou, China, in 2010, and the M.Phil. and Ph.D. degrees in electronic and computer engineering from the Hong Kong University of Science and Technology (HKUST), Hong Kong, in 2012 and 2015, respectively. In 2015, he joined HKUST as a Postdoctoral Researcher and led the HKUST-Massachusetts Institute of Technology (MIT) consortium project on wireless sensing

node design for smart green building applications. He was with MIT in 2016, worked on low-power data converter design for this project. In 2017, he joined Hamad Bin Khalifa University as a Founding Faculty Member, where he is currently an Assistant Professor with the Division of Information and Computing Technology, College of Science and Engineering. His research interests include the design of energy-efficient analog/mixed-signal circuits, sensor/sensor interface, and heterogeneous integrated systems for *in vitro/vivo* healthcare. He was a recipient of the IEEE ASP-DAC Best Design Award in 2016.



Amine Bermak (Fellow, IEEE) received the master's and Ph.D. degrees in electrical and electronic engineering from Paul Sabatier University, France, in 1994 and 1998, respectively. He has held various positions in academia and industry in France, U.K., Australia, and Hong Kong. He is currently a Professor and the Associate Dean of the College of Science and Engineering, Hamad Bin Khalifa University. He has published over 400 articles, designed over 50 chips, and graduated 25 Ph.D. and 20 M.Phil. students.

For his excellence and outstanding contribution to teaching, he was nominated for the 2013 Hong Kong UGC Best Teacher Award (for all HK Universities). He was a recipient of the 2011 University Michael G. Gale Medal for distinguished teaching. He was also a two-time recipient of the Engineering Teaching Excellence Award in HKUST for 2004 and 2009. He received six distinguished awards, including the Best University Design Contest Award at ASP-DAC 2016, the Best Paper Award at IEEE ISCAS 2010, the 2004 IEEE Chester Sall Award, and the Best Paper Award at the 2005 International Workshop on SOC for Real-Time Applications. He has served on many editorial boards and is an editor for IEEE TRANSACTIONS ON VERY LARGE SCALE INTEGRATION (VLSI) SYSTEMS, the IEEE TRANSACTIONS ON ELECTRON DEVICES (TED), and *Scientific Reports* (Nature). He is an IEEE Distinguished Lecturer.